Available online at www.sciencedirect.com
ScienceDirect
Journal of Nutritional Biochemistry 21 (2010) 381–389
Journal of Nutritional Biochemistry

Astaxanthin protects mitochondrial redox state and functional integrity against oxidative stress

Alexander M. Wolf[a], Sadamitsu Asoh[a], Hidenori Hiranuma[a], Ikuroh Ohsawa[a,b], Kumiko Iio[c], Akira Satou[c], Masaharu Ishikura[c], Shigeo Ohta[a,*]

[a]Department of Biochemistry and Cell Biology, Institute of Development and Aging Sciences, Nippon Medical School, Nakahara-ku, Kawasaki, Kanagawa 211-8533, Japan
[b]The Center of Molecular Hydrogen Medicine, Institute of Development and Aging Sciences, Nippon Medical School, 1-396 Kosugi-cho, Nakahara-ku, Kawasaki, Kanagawa 211-8533, Japan
[c]Life Science Institute, Yamaha Motor Co. Ltd., 3001-10 Kuno, Fukuroi, Shizuoka 437-0061, Japan

Received 6 August 2008; received in revised form 8 January 2009; accepted 12 January 2009

Abstract

Mitochondria combine the production of energy with an efficient chain of reduction–oxidation (redox) reactions but also with the unavoidable production of reactive oxygen species. Oxidative stress leading to mitochondrial dysfunction is a critical factor in many diseases, such as cancer and neurodegenerative and lifestyle-related diseases. Effective antioxidants thus offer great therapeutic and preventive promise. Investigating the efficacy of antioxidants, we found that a carotenoid, astaxanthin (AX), decreased physiologically occurring oxidative stress and protected cultured cells against strong oxidative stress induced with a respiratory inhibitor. Moreover, AX improved maintenance of a high mitochondrial membrane potential and stimulated respiration. Investigating how AX stimulates and interacts with mitochondria, a redox-sensitive fluorescent protein (roGFP1) was stably expressed in the cytosol and mitochondrial matrix to measure the redox state in the respective compartments. AX at nanomolar concentrations was effective in maintaining mitochondria in a reduced state. Additionally, AX improved the ability of mitochondria to remain in a reduced state under oxidative challenge. Taken together, these results suggest that AX is effective in improving mitochondrial function through retaining mitochondria in the reduced state.

Keywords: Oxidative stress; Mitochondrial membrane potential; Oxygen consumption; Redox-sensitive GFP; Astaxanthin; Metabolic syndrome

1. Introduction

Oxidative stress is involved in the pathogenesis of atherosclerosis [1,2], cancer [3], diabetes [4,5], neurodegenerative [6–8] and other diseases, as well as in the aging process itself. Antioxidant treatment has therefore great promise in alleviating some of the detrimental effects of oxidative stress [9], and several types of antioxidants stimulate lipid oxidation, which may have merit in improving metabolic syndrome [10–12]. A huge selection of both natural and synthetic antioxidants is available and can be ingested easily with, in the case of food-derived antioxidants, little concern about adverse side effects. This attractiveness has on one hand led a multi-billion dollar supplement industry often based on anecdotal evidence [13,14] and, on the other hand, to large-scale clinical trials to determine efficacy, often with disappointing results [15,16]. Selecting the most promising substances is therefore important to avoid costly failures [17].

Cellular reduction–oxidation (redox) state is directly affected in conditions of oxidative stress, and depletion of endogenous antioxidants plays a critical role in disease progression [18]. Genetically encoded indicators can be targeted to specific organelles of interest and expressed in a wide variety of cells and organisms [19]. The indicator used in this work, redox-sensitive green fluorescent proteins (roGFP1), allows the real-time visualization of the oxidation state of the indicator [20,21]. In roGFP1 (GFP with mutations C48S, S147C, and Q204C), two surface-exposed cysteines are placed at Positions 147 and 204 on adjacent β-strands close to the chromophore. Disulfide formation between the cysteine residues promotes protonation of the chromophore and increases the excitation spectrum peak near 400 nm at the expense of the peak near 490 nm. The ratios of fluorescence from excitation at 400 and 490 nm indicate the extent of oxidation and thus the redox potential while canceling out the amount of indicator and the absolute optical sensitivity [20,21]. In contrast to its close cousin roGFP2, roGFP1 also offers the advantage to be insensitive to variations in pH [21].

Abbreviations: AX, astaxanthin; CCD, charge-coupled device; DCF, 2′,7′-dichlorofluorescein; DMEM/F12, Dulbecco's modified Eagle medium/F-12 nutrient mixture; DNP, 2,4-dinitrophenol; FBS, fetal bovine serum; GFP, green fluorescent protein; H_2DCFDA, 2′,7′-dichlorodihydrofluorescein diacetate; JC-1, 5,5′,6,6′-tetrachloro-1,1′,3,3′-tetraethylbenzimidazolylcarbocyanine iodide; N.A., numerical aperture; PBS, phosphate buffered saline; roGFP, redox-sensitive green fluorescent protein; TMRM, tetramethyl rhodamine methyl ester.

* Corresponding author. Tel.: +81 44 733 9267; fax: +81 44 733 9268.
E-mail address: ohta@nms.ac.jp (S. Ohta).

0955-2863/$ – see front matter © 2010 Elsevier Inc. All rights reserved.
doi:10.1016/j.jnutbio.2009.01.011

Astaxanthin (AX), a red-orange carotenoid pigment, is a powerful antioxidant that occurs naturally in a wide variety of living organisms and has positive effects on cancer, diabetes, the immune system, and ocular health [22]. Health benefits such as cardiovascular disease prevention, immune system boosting, bioactivity against *Helicobacter pylori*, and cataract prevention have been associated with AX [23]. Oral supplementation of a synthetic AX derivative reduced lipid peroxidation levels and provided significant cardioprotection, consistent with its lipophilic nature and in vitro antioxidant properties [24]. However, the concentrations of AX used in these studies were generally much higher than what can be achieved using supplementation [25] or dietary intervention [26]. We investigated how AX could exert an antioxidant effect in a concentration range chosen close to what can be achieved using supplements and/or diet.

2. Materials and methods

2.1. Cell culture

HeLa human cervical cancer cells were maintained in Dulbecco's modified Eagle medium/F-12 nutrient mixture (DMEM/F12) medium (Invitrogen Japan K.K.) supplemented with 10% fetal bovine serum (FBS). Undifferentiated PC12 rat pheochromocytoma cells were cultured in DMEM supplemented with 10% FBS and 5% heat-inactivated horse serum. Jurkat immortalized T lymphocyte cells were cultivated in RPMI1640 (Invitrogen) containing 10% FBS. All media contained 100 U/ml penicillin and 100 μg/ml streptomycin, and all cell types were maintained at 37°C in a humidified atmosphere of 5% CO_2 and 95% air.

2.2. Transfection

HeLa cells were transfected with the mammalian expression vector pEGFP-N1 (Clontech, Takara Bio, CA) containing roGFP1 (for expression in the cytosol) or roGFP1 with a mitochondrial targeting sequence (pyruvate dehydrogenase E1 subunit leader sequence, for expression in mitochondria) using the Effectene Transfection Reagent (Qiagen Japan) according to the manufacturer's protocol. Stable transfectants were selected using 400 μg/ml Geneticin (Invitrogen) for more than 4 weeks and cloned. Expression of roGFP1 was confirmed by its fluorescence.

2.3. Cell viability

Antimycin A (Sigma) was dissolved to 50 mg/ml in dimethyl sulfoxide (DMSO). The medium was changed to DMEM supplemented with 1.0% FBS overnight, and the PC12 cells were then treated with AX (Sigma) at the indicated concentrations for 6 and 24 h in DMEM supplemented with 1.0% FBS. After AX treatment, 20 μg/ml antimycin A was added (final DMSO concentration: 0.1%) and the cells incubated for 20 h. The number of live/dead cells was counted with a fluorescence microscope (Nikon AZ100, Tokyo) using the LIVE/DEAD cell viability kit for mammalian cells (Invitrogen) and the survival rate expressed as live cells/(live cells+dead cells).

2.4. Fluorescence microscopy

Fluorescence images were recorded using a multidimensional imaging workstation (AS MDW, Leica Microsystems, Wetzlar, Germany) consisting of a tunable light source (Polychrome IV monochromator, Till Photonics, Gräfelfing, Germany), an inverted epifluorescence microscope (DM IRE2, Leica Microsystems) contained in a climate chamber maintained at 37°C and a cooled charge-coupled device (CCD) camera (CoolSnap HQ, Roper Scientific, Princeton, NJ). A 0.35× demagnifiying lens (Leica Microsystems) was inserted between the microscope and the CCD camera. The components were controlled by custom-made software written in C (Bloodshed Dev-C ++) and LabVIEW (National Instruments, Austin, TX).

2.5. Redox-sensitive fluorescent protein fluorescence recording

HeLa cells expressing roGFP1 were washed with PBS and fluorescence recorded. Hydrogen peroxide was diluted from a 30% (w/v) stock solution with phosphate buffered saline (PBS) (37°C) to 500 μM and added to reach the indicated concentration. Dual excitation ratio imaging was performed using a 20× objective [numerical aperture (N.A.) 0.5] and 800 ms exposure time at 410 and 490 nm excitation wavelength. A 500-nm short pass excitation filter (E500SP), 515 nm extended-range dichroic mirror (515DCXR) and 520–600 nm bandpass emission filter (HQ560/80, all from Chroma Technology Corporation, Rockingham, VT) was used for both wavelengths.

Fluorescence data were analyzed using MATLAB (MathWorks, Version 7 Release 14, Natick, MA). After subtracting background fluorescence and CCD dark field, areas corresponding to cells were automatically selected using the criteria of more than 10 connected pixels with fluorescence intensity above both 3% of the maximum fluorescence in the field of view and more than 8 standard deviations above the background noise/intensity in the image obtained with 410 nm excitation wavelength. Such regions were marked and visually confirmed to correspond to cells expressing fluorescent protein. The fluorescence ratio was formed by dividing the fluorescence integral of such regions at 410 and 490 nm excitation. When following the time course of the fluorescence ratio of individual cells, in order to be counted, cells had to fulfill the above criteria at every recorded time point.

2.6. Mitochondrial membrane potential

A 0.5-mM stock solution of 5,5′,6,6′-tetrachloro-1,1′,3,3′-tetraethylbenzimidazolylcarbocyanine iodide (JC-1; Invitrogen) was prepared in equal volumes of ethanol and DMSO. HeLa cells were cultured in DMEM/F12+10% FBS with or without 800 nM AX (control: DMSO) for 6 h, 1 day and 2 days, then stained with 250 nM JC-1 in culture medium for 60 min, washed with PBS and fluorescence recorded immediately, all at 37°C. Dual excitation ratio imaging was performed using a 20× objective (N.A. 0.5) and 200 ms exposure time at 520 nm and 570 nm excitation wavelength. A 580 nm short pass excitation filter (E580SP), 585 nm extended range dichroic mirror (585DCXR) and 590- to 670-nm bandpass emission filter (HQ635/60, all from Chroma Technology Corporation) was used for both excitation wavelengths. Fluorescence data was analyzed using MATLAB (MathWorks, Version 7 Release 14). After subtracting background (dark field) fluorescence, areas corresponding to cells were automatically selected using the criteria of more than 10 connected pixels with fluorescence intensity above both 3% of the maximum fluorescence in the field of view and more than 8 standard deviations above the background noise/intensity in the image obtained with 520 nm excitation wavelength. The fluorescence ratio was formed by dividing the fluorescence integral of all such regions at 570 nm and 520 nm excitation. The field of view usually contained about 100 to 200 cells.

2.7. Superoxide measurement

HeLa cells were cultured in DMEM/F12+10% FBS with or without 800 nM AX (control: DMSO) for 6 h, 1 day and 2 days, then exposed to 30 μg/ml antimycin A for 15 min, then 250 nM MitoSOX Red (Invitrogen) and 500 nM Hoechst34580 (Invitrogen) added and incubated for 60 min, and fluorescence recorded using a 20× (N.A. 0.5) objective. Hoechst34580 fluorescence was excited at 395 nm in combination with a 500-nm short-pass excitation filter (E500SP), 515 nm extended-range dichroic mirror (515DCXR) and 520–600 nm bandpass emission filter (HQ560/80). Ethidium (MitoSOX Red oxidation product) fluorescence was excited at 520 nm and recorded using a 580-nm short-pass excitation filter (E580SP), 585 nm extended range dichroic mirror (585DCXR) and 590–670 nm bandpass emission filter (HQ635/60). Fluorescence data was analyzed using MATLAB (MathWorks, Version 7 Release 14). After subtracting background (dark field) fluorescence, cell nuclei were automatically detected using the criteria of more than 25 connected pixels with fluorescence intensity above both 20% of the maximum fluorescence in the field of view and more than 10 standard deviations above the background noise/intensity in the Hoechst 34580 image. Mean ethidium fluorescence intensity in the area above the nucleus was used as the measure of superoxide production.

2.8. Flow cytometry

Jurkat cells were cultivated in medium in the presence or absence (DMSO) of AX (800 nM) for 6 h, 1 day and 2 days without medium change. There was no difference among the growth rates of these cell cultures. For detection of superoxide anion, cells were incubated with antimycin A (30 μg/ml) for 10 min. Then, MitoSOX Red (250 nM) was added. After 1 h, the cells were analyzed by flow cytometry (Cell Lab Quanta system, Beckman Coulter, Chaska, MN). For detection of hydroxyl peroxides, cells were incubated with 2′,7′-dichlorodihydrofluorescein diacetate (H_2DCFDA) (20 μM, Invitrogen). After 15 min, antimycin A (30 μg/ml) was added. One hour later, the cells were analyzed by flow cytometry as above. Ten thousand cells of normal size (assessed by forward scattering) were analyzed under each condition.

2.9. Physiologically occurring (basal) oxidative stress

Cells were cultured in DMEM/F12+10% FBS with or without 800 nM AX (control: DMSO) for 2 days then incubated with 20 μM H_2DCFDA and 500 nM Hoechst34580 in medium for 60 min, washed with PBS and the dichlorofluorescein (DCF) fluorescence of individual cells measured immediately afterward using a 20× objective (N.A. 0.5). Fluorescence was recorded using the BGR triple bandpass filter set (Leica Microsystems). Hoechst34580 was excited at 403 nm and DCF at 496 nm wavelength. Fluorescence data were analyzed using MATLAB (MathWorks, Version 7 Release 14). After subtracting background (dark-field) fluorescence, cell nuclei were automatically detected using the criteria of more than 25 connected pixels with fluorescence intensity above both 5% of the maximum fluorescence in the field of view and more than 10 standard deviations above the background noise/intensity in the Hoechst 34580 image. Mean DCF fluorescence intensity in the area above the nucleus was used as the measure of oxidative stress.

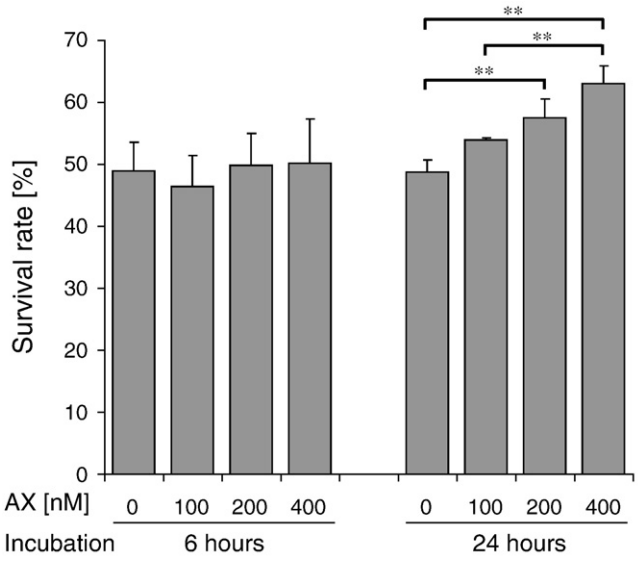

Fig. 1. Astaxanthin effect on PC12 cell survival under oxidative stress. Cells were cultured in the presence of 0, 100, 200 and 400 nM AX for 6 h or 24 h and then exposed to 30 μg/ml antimycin A as described under cell viability in Materials and methods. No effect was detected when cells were preincubated with AX for 6 h. When preincubated with AX for 24 h, cells were protected against cell death induced by oxidative stress, significantly for 200 and 400 nM AX ($P<.01$). Data are means±S.D. from three fields containing 100–200 cells each.

2.10. Oxygen consumption

HeLa cells were cultured in DMEM/F12+10% FBS with or without 800 nM AX (control: DMSO) for 6 h, 1 day and 2 days, trypsinized and resuspended in DMEM/F12. Oxygen consumption was measured using the Oxygen Meter Model 781 and the Mitocell MT200 closed respiratory chamber (Strathkelvin Instruments, North Lanarkshire, UK), continuously stirred at 37°C. The oxygen respiration rate was calculated in the following three conditions: basal rate (no additions), State 4 [after addition of 2 μM oligomycin (Sigma)], uncoupled [after addition of 80 μM 2,4-dinitrophenol (DNP); Sigma] using the Strathkelvin 949 Oxygen System software. Cell concentration was determined using a hemocytometer.

2.11. Confocal microscopy

To confirm targeting of roGFP1 to the mitochondrial matrix, HeLa cells expressing the mitochondrial targeting vector were cultured in a glass-bottom dish and stained with 40 nM tetramethyl rhodamine methyl ester (TMRM, Molecular Probes, Invitrogen) for 20 min. Fluorescence was observed using a FluoView FV300 confocal microscope (Olympus, Tokyo, Japan) with a 60× (N.A. 1.4) oil immersion objective. roGFP1 was excited at 488 nm and emission collected above 510 nm, while TMRM was excited at 543 nm and emission collected above 570 nm.

2.12. Statistical calculations

Statistical significance was determined using the unpaired two-tailed Student's *t* test in Excel (Microsoft, Redmond, WA) or one-way analysis of variance (ANOVA) followed by a Tukey–Kramer multiple comparison test in Matlab (MathWorks, Version 7 Release 14). Error bars indicate the standard deviation of three or more measurements. The number of asterisks indicates statistical significance. Specifically, * indicates $P<.05$, ** indicates $P<.01$ and *** indicates $P<.001$.

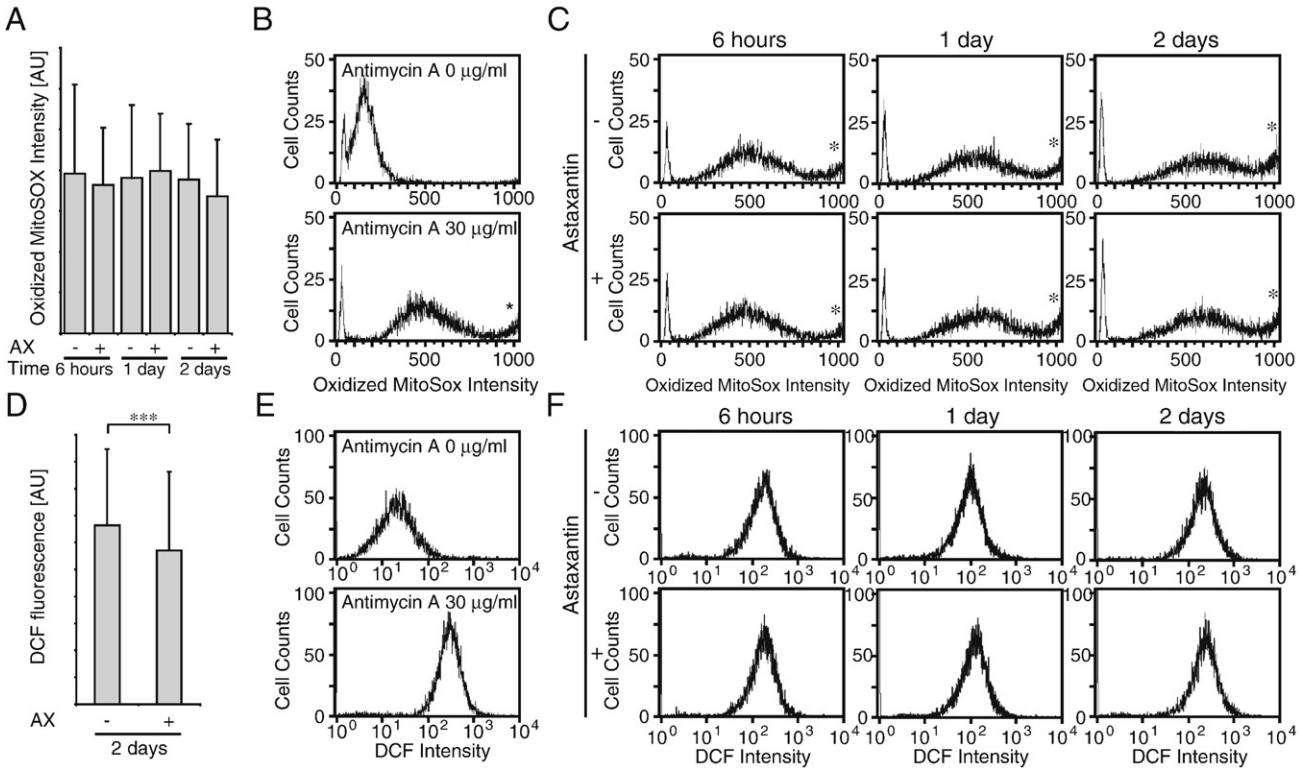

Fig. 2. Superoxide and oxidative stress. (A) PC12 cells were preincubated with AX for indicated periods, followed by exposure to antimycin A to induce superoxide. Superoxide, as measured using MitoSOX Red, was not changed significantly by culturing cells with AX. Data were obtained as the means±S.D. by quantifying signal intensities of 70–100 cells. (B) Superoxide production is induced by incubating Jurkat cells with 30 μg/ml antimycin A. (C) Jurkat cells cultivated in the presence or absence (DMSO) of AX (800 nM) for 6 h, 1 day, and 2 days were treated with antimycin A (30 μg/ml). No significant difference in the amount of oxidized MitoSOX Red was observed, indicating that, under conditions of oxidative stress and at a concentration of 800 nM, AX is unable to scavenge significant amounts of superoxide. (D) Basal oxidative stress level in cells, as measured by incubating cells with H_2DCFDA. AX significantly decreased the amount of DCF produced in HeLa cells incubated with AX for 2 days ($n=383$ cells, control: $n=403$ cells; from three independent experiments under each condition). *** $P<.001$. (E) Antimycin A (30 μg/ml) also induced acute oxidative stress as assessed using H_2DCFDA. The amount of DCF produced was increased more than 10-fold. (F) Similar to C, AX did not reduce acute oxidative stress. No significant difference in the amount of DCF was observed.

3. Results

3.1. AX improves cell survival under oxidative stress

To test whether AX protects cells against oxidative stress, we exposed rat adrenal pheochromocytoma (PC12) cells, a neuronal model cell line shown to be sensitive to oxidative stress [27], to antimycin A. Antimycin A, an inhibitor of complex III of the electron transport chain, induces oxidative stress by increasing mitochondrial superoxide production [28] (see also Fig. 2B and E). Preincubation with AX for 6 h did not significantly increase PC12 cell survival, but when cells were exposed to AX for 24 h, a significant increase in the number of surviving cells was observe with more than 200 nM AX, demonstrating that AX was able to protect PC12 cells against oxidative stress at relatively low concentrations (Fig. 1). The effect was concentration dependent, with 400 nM AX being more protective than 100 nM AX ($P<.01$).

3.2. AX reduces basal oxidative stress levels but not acute oxidative stress

To determine the mechanism by which AX protects against oxidative stress, we determined whether AX was able to directly scavenge superoxide radical. Human cervical cancer (HeLa) and T lymphocyte (Jurkat) cells were exposed to antimycin A as an acute stress model, and oxidation of the superoxide-sensitive probe MitoSOX Red quantified as described in Materials and methods. Preincubation of cells with 800 nM AX did not significantly reduce the

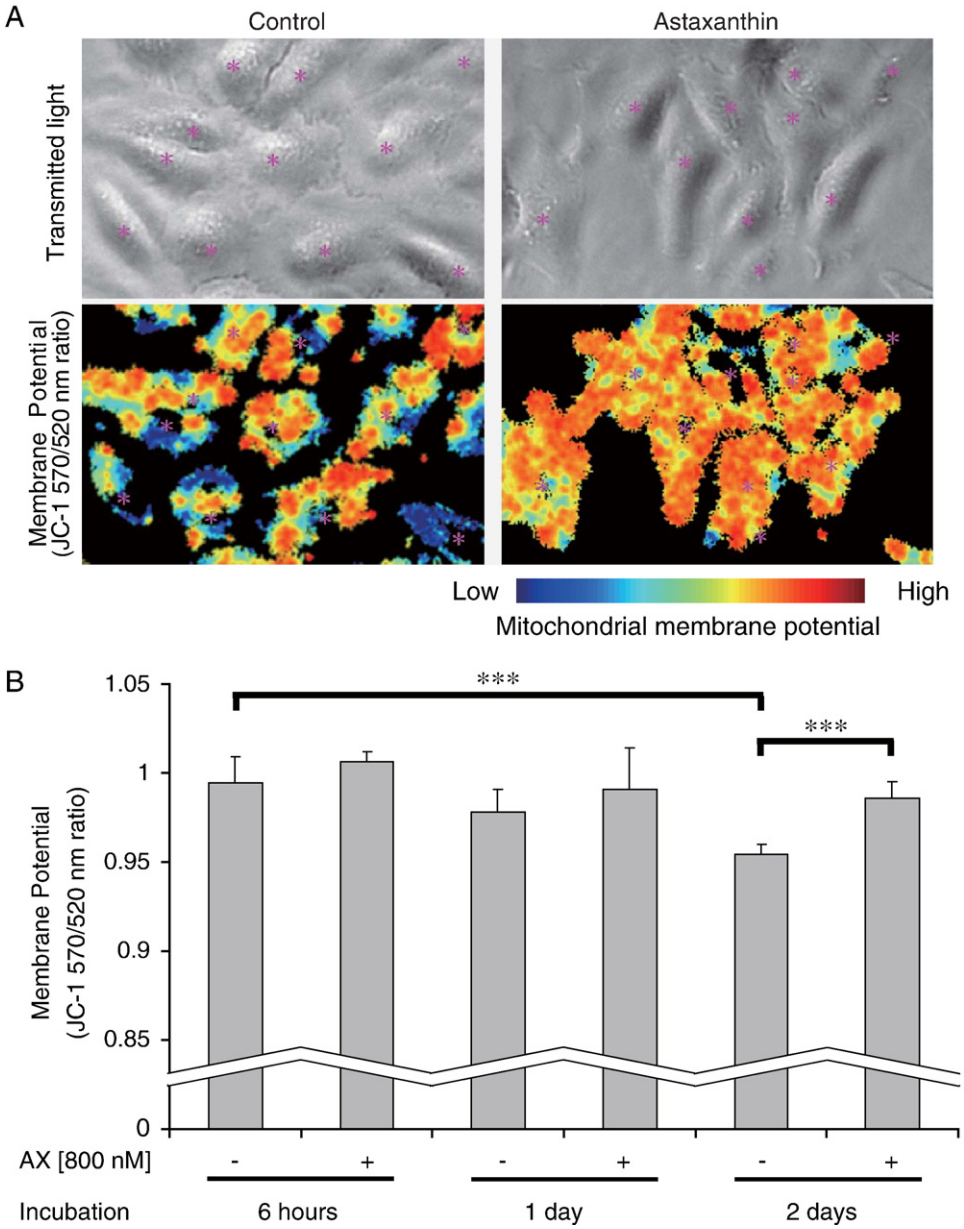

Fig. 3. Mitochondrial membrane potential. (A) Representative transmitted light (upper row) and membrane potential (lower row) images of HeLa cells cultured for 2 days in the presence (right) or absence (left) of 800 nM AX. The membrane potential image was created by color coding the dual excitation fluorescence ratio. Asterisks (pink) mark the approximate positions of cell nuclei. (B) Average JC-1 dual excitation fluorescence ratio from three independent experiments, with fluorescence recorded at 2 locations for each experiment. Membrane potential was significantly higher ($P<.001$) in the presence of AX after 2 days in culture, but rather than increasing the mitochondrial membrane potential, AX seemed to prevent a loss of membrane potential that occurred with increasing time in culture.

amount of superoxide detected (Fig. 2A), suggesting that AX did not scavenge excess amounts of superoxide under this unphysiological condition. Similarly, Jurkat cells were treated with antimycin A-generated superoxide anion (as assessed by MitoSOX Red) and reactive peroxides (as assessed by H_2DCFDA) to a great extent (Fig. 2B and E). In these flow cytometry experiments, the population of cells with an intensity of 1000 or more (marked with * in Fig. 2B and C) was between 2% and 4% of the cells analyzed. Quantitative analysis revealed no significant difference in the fluorescence intensity of oxidized MitoSOX product (Fig. 2C) or DCF (Fig. 2F) between AX-treated or nontreated cells, even when cells were treated with AX for 2 days. Post-addition of AX did not change fluorescent patterns of the antimycin A-treated cells without AX treatment (data not shown), indicating that AX does not interfere with fluorescence of oxidized MitoSOX and DCF.

However, when the basal level of oxidative stress, that is the physiologically occurring oxidative stress, in HeLa cells was determined using the oxidant sensitive probe 2′,7′-dichlorodihydrofluorescein, AX significantly reduced the amount of fluorescent oxidation product (DCF) produced (Fig. 2D), indicating that AX is able to reduce endogenous oxidative stress. This signifies that there is a low but detectable amount of endogenous oxidative stress under normal culture conditions, which AX can reduce.

3.3. AX helps maintain the mitochondrial membrane potential

We proceeded to determine whether such endogenous oxidants affect cellular function and whether AX could influence it. The mitochondrial membrane potential was quantified using the aggregate-forming probe JC-1 [29]. Using dual excitation ratio imaging, we observed a significantly higher mitochondrial membrane potential when AX was present in culture after 2 days (Fig. 3A). For shorter incubation times, the difference was not significant. Interestingly, rather than increasing the mitochondrial membrane potential, AX seemed to slow down a gradual loss of membrane potential that may occur with time in culture. While a significant loss in the membrane potential occurred from 6 h to 2 days in culture without AX (Fig. 3B, $P<001$), no significant difference/loss could be detected in the presence of AX.

3.4. AX effect on respiratory control

Speculating that a decrease in mitochondrial membrane could also affect mitochondrial respiration, we measured the oxygen consumption of intact HeLa cells cultured under the same conditions. Measuring first baseline oxygen consumption (no additions), then the mitochondrial State 4 consumption (by blocking complex V with oligomycin) and then maximal oxygen consumption by uncoupling mitochondria with DNP (80 μM) (Fig. 4A), we could not observe significant changes in the absolute consumption rates (Fig. 4B), but the ratio of baseline to uncoupled oxygen consumption was significantly higher in the presence of AX, that is, mitochondria were more active in the presence of AX (Fig. 4C). In addition, the relative reduction in oxygen consumption upon addition of oligomycin was increased in the presence of AX (Fig. 4C). Together, these findings suggest that AX stimulates respiration probably by maintaining a higher membrane potential (Fig. 3).

3.5. AX improves the mitochondrial redox state

Due to these positive but rather subtle effects of AX on mitochondrial function, we looked for a sensitive method to detect relatively mild oxidative stress at the organelle level. We chose redox-sensitive GFP as a promising method since it is ratiometric and can be targeted to various cellular compartments [20,21,30]. Furthermore, it has been shown to be a quantitative sensor for the redox potential of the cellular glutathione redox buffer [31]. HeLa

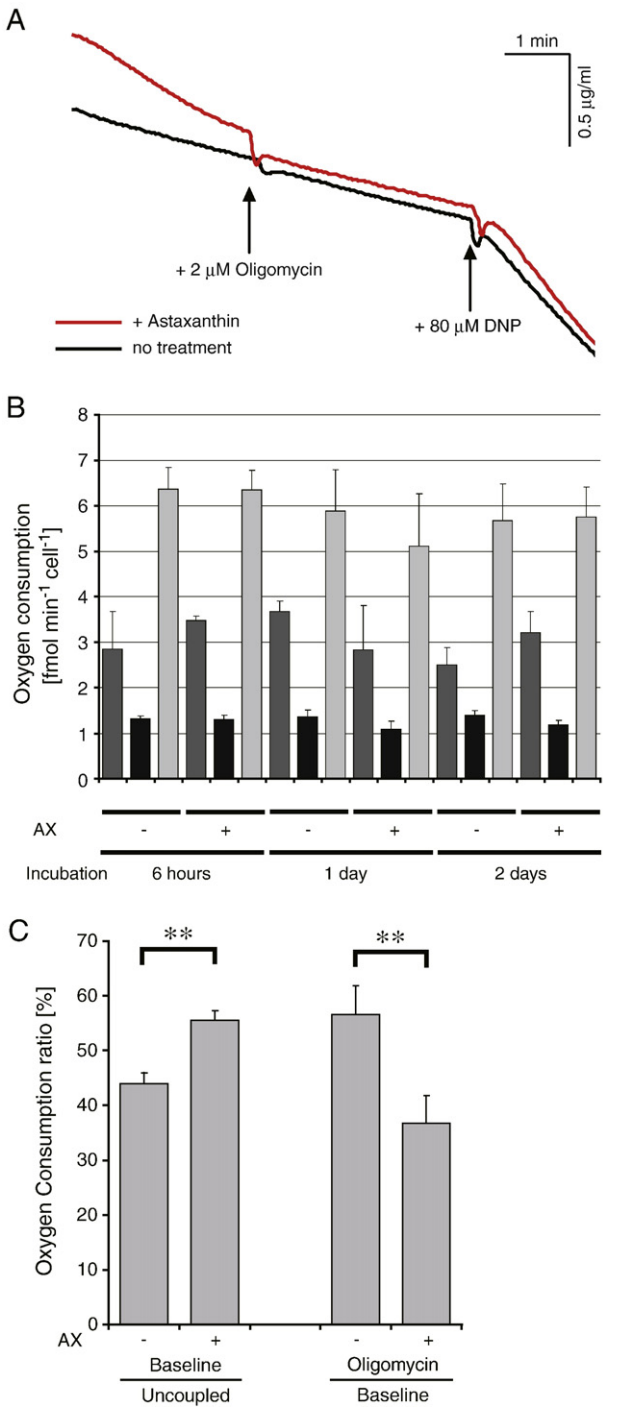

Fig. 4. Oxygen consumption profiles. (A) Representative traces of the oxygen consumption of intact HeLa cells cultured with (800 nM, red trace) or without (black trace) AX. Oligomycin and DNP were added at the indicated (arrows) time points. (B) Average oxygen consumption per cell under baseline conditions (BL; dark gray bars), in the presence of 2 μM oligomycin (+OM; black bars) and when uncoupled with 80 μM DNP (+DNP, light gray bars). Data are the average±S.D. of three measurements of cells cultured for 6 h (6H), 1 day (1D) or 2 days (2D) in the presence or absence of 800 nM AX (control: DMSO). (C) AX increased the ratio of baseline divided by uncoupled oxygen consumption and decreased the ratio of oxygen consumption in the presence of oligomycin divided by baseline oxygen consumption. Data are mean±S.D. ** $P<01$.

cells were stably tranfected with the expression vector for roGFP1 targeted to mitochondria as described above and the colocalization of roGFP1 with mitochondria confirmed using confocal microscopy. RoGFP1 showed almost perfect overlap with the mitochondrial marker dye TMRM (Fig. 5A). Cells expressing mitochondrial roGFP1 showed no abnormal morphology (Fig. 5A and B), and mitochondria exhibited the characteristic tubular shape and movement presumably along microtubules (Supplementary Movie). The mitochondrial redox state of individual cells was measured using dual excitation imaging (Fig. 5C). Mitochondrial roGFP1 (basal redox state) was more reduced in cells cultured with AX for 6 h, 1 day and 2 days (Fig. 5D and E). Mitochondrial ability to maintain the reducing

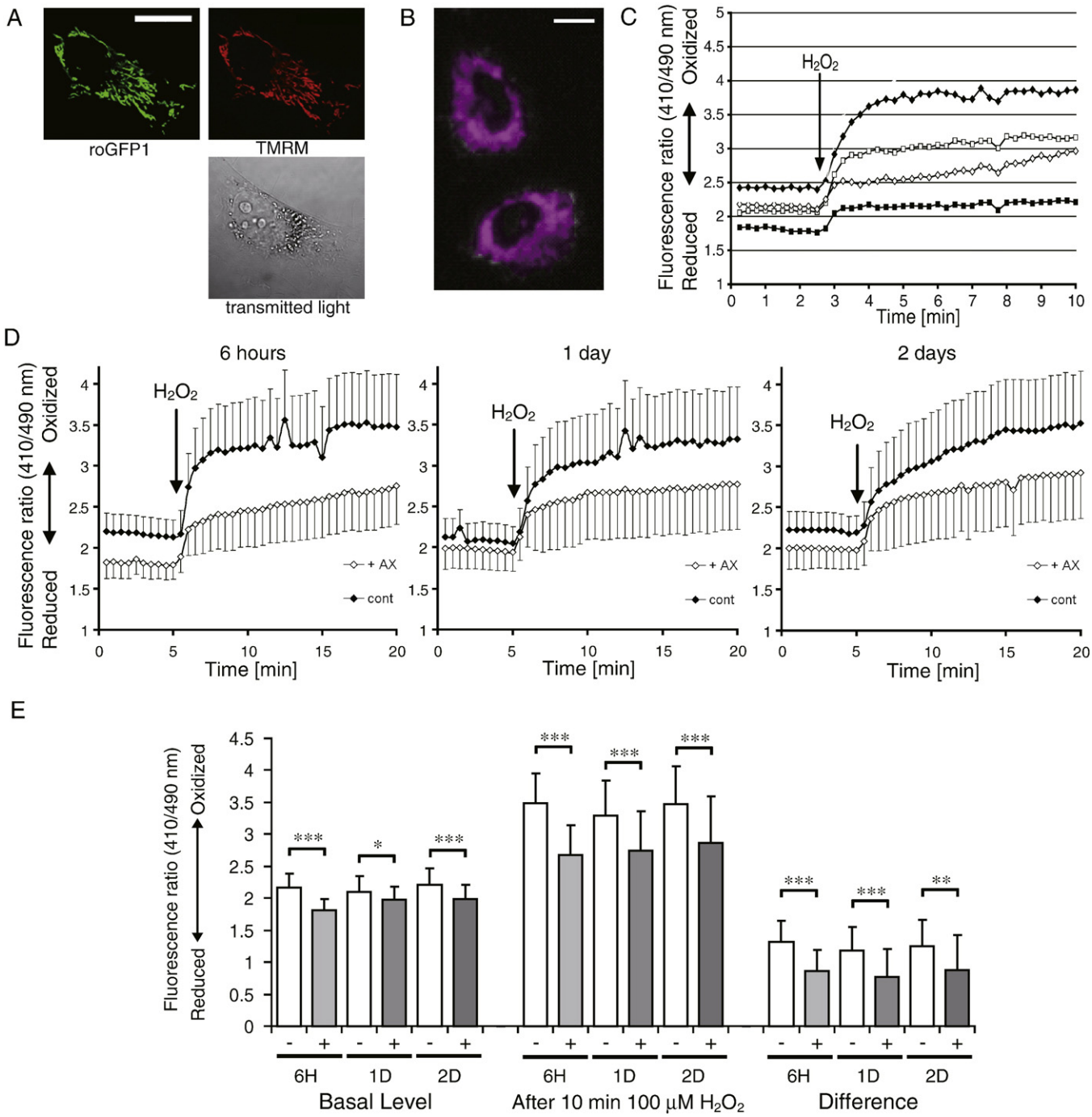

Fig. 5. Mitochondrial redox state measured using redox-sensitive GFP. (A) Confocal and transmitted light images of a HeLa cell expressing roGFP1 targeted to mitochondria. Overlap of TMRM and roGFP1 fluorescence confirms mitochondrial localization of roGFP1. Scale bar: 20 µm. (B) Epifluorescence image of HeLa cells expressing roGFP1 targeted to mitochondria. Regions automatically selected for analysis are marked in pink. Scale bar: 20 µm. (C) Representative traces of the roGFP1 redox state time course (dual excitation fluorescence ratio). Four individual cells show the heterogeneity of mitochondrial redox state between cells. After the indicated periods, 100 µM hydrogen peroxide was added (arrow). (D) Average time course indicating mitochondrial redox state of cells cultured with or without 800 nM AX for 6 h (6H) (+AX: n=35 cells, control: n=34 cells), 1 day (1D) (+AX: n=41 cells, control: n=32 cells) or 2 days (2D) (+AX: n=32 cells, control: n=27 cells). Average baseline as well as redox state after addition of 100 µM hydrogen peroxide (arrow) was more reduced when AX was present. (E) Average baseline fluorescence ratio, ratio after addition of hydrogen peroxide and amount of oxidation (ratio difference) induced by hydrogen peroxide were significantly lower, that is, reduced when AX was present. Data are mean±S.D. *P<.05, **P<.01, ***P<.001.

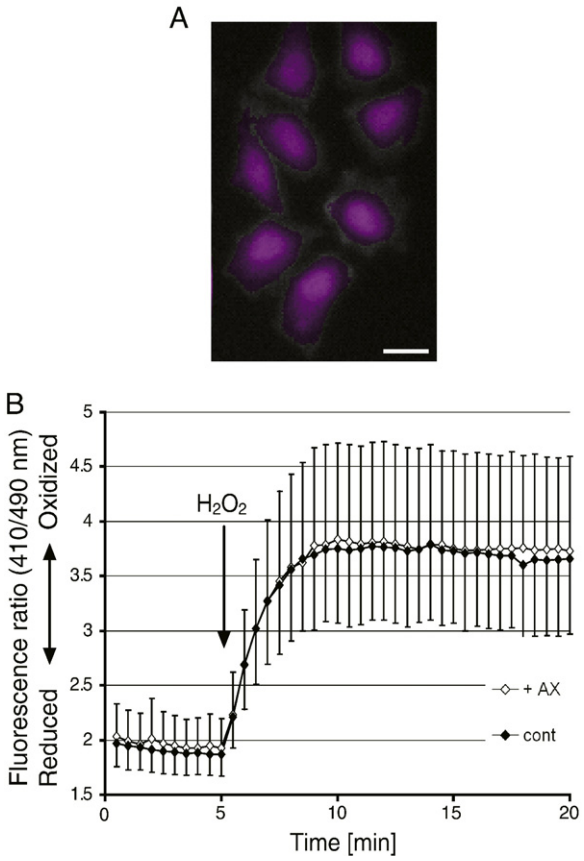

Fig. 6. Effect of AX on the cytosol redox state. (A) Epifluorescence image of HeLa cells expressing roGFP1 in the cytosol. Regions automatically selected for analysis as individual cells are marked in pink. Scale: 20 μm. (B) Time course of cytosol redox state (410/490 nm dual excitation fluorescence ratio) upon addition of 100 μM H_2O_2 (arrow). No difference was detected, neither in the basal redox state nor in the change or state after addition of H_2O_2, between cells cultured for 2 days in the presence (open diamonds, n=73 cells) or absence (filled diamonds, n=90 cells) of 800 nM AX.

environment was then tested by exposing cells to 100 μM H_2O_2, which quickly oxidized mitochondrial roGFP1 but significantly less so when AX was present (Fig. 5D and E). To exclude the possibility that the more reduced state after addition of H_2O_2 is simply a consequence of the more reduced (basal) state prior to addition of H_2O_2, we also compared the change in fluorescence ratio induced by H_2O_2. This difference was also significantly smaller in the presence of AX (Fig. 5E). Whether this antioxidant effect of AX was limited to mitochondria or also extended to the cytosol was tested using cells expressing roGFP1 in the cytosol (Fig. 6A). The basal redox state and resistance to oxidative challenge with H_2O_2 were tested in the same manner as for mitochondria, but no effect of AX on the redox state of the cytosol could be detected (Fig. 6B).

4. Discussion

The results above demonstrate that, under basal conditions, AX had a small but significant positive effect on mitochondrial function (higher membrane potential, higher respiratory control). This is reassuring since endogenous oxidative stress, though clearly present [32], should be rather mild in the absence of external stress-inducing agents. Since mitochondria are a major source of reactive oxygen species (ROS) in the cell, accumulation of AX in the mitochondrial membrane would potentiate its antioxidant effects. There is a report showing AX protects mesangial cells from hyperglycemia-induced oxidative signaling [33]. The fact that AX was able to maintain mitochondria but not the cytosol in a reduced state (Fig. 5) indicates that the effect of AX is, at least during mild, endogenous oxidative stress, concentrated on mitochondria. The effect of AX became more pronounced with incubation time. Interestingly, such a time dependency was also observed in an investigation of the antitumor activity of AX [34]. AX, at a total serum concentration of approximately 1.2 μM, suppressed tumor cell growth when mice were fed AX before inoculation but was ineffective when the AX-supplemented diet was started at the same time as tumor inoculation [34].

Cell types differ in their dependence on mitochondria-generated ATP as a source of energy and in their sensitivity to oxidative stress. AX protected PC12 cells against antimycin A-induced cell death. HeLa cells, in contrast, can rely on glycolysis as the sole energy supply and survive even in the absence of a functional electron transport chain [35]. Accordingly, blocking electron transport with antimycin A, though clearly inducing oxidative stress, does not necessarily lead to HeLa cell death [36,37]. That AX was protective in both cells lines indicates that the effect of AX should not be cell type or cancer specific [38]. Moreover, mitochondria isolated from PC12 cells had oxygen consumption rates similar to isolated rat liver mitochondria (data not shown) [39], indicating that the effects of AX described here are not specific to those of cancer-type cells.

Although direct superoxide scavenging by a highly water-dispersible carotenoid phospholipid has been reported at high concentrations [40], AX may not exert its strong effect by scavenging superoxide. In fact, under conditions of acute oxidative stress when large amounts of ROS are produced, AX showed no detectable effect, indicating that the effects of AX are not due direct scavenging of ROS such as superoxide or peroxides (Fig. 2A). This is to be expected since superoxide is a charged radical unable to cross cellular membranes and carotenoids are extremely lipophilic. On the other hand, since AX reduced the endogenous oxidative stress level (Fig. 2D), it is reasonable to assume it protects cells against oxidative damage in the lipid phase (Fig. 1). Thus, even though it may not scavenge ROS directly, AX has the potential to protect cells against damage mediated by oxidative stress. Since ROS including superoxide and hydrogen peroxide play significant roles in the signal transduction at low concentrations [41], this characteristic of AX suggests little possibilities of negative side effects of AX consumption.

The increase in mitochondrial oxygen consumption of AX-treated cells is probably in part a consequence of the change in mitochondrial membrane potential [41]. The relatively higher reduction in oxygen consumption upon addition of oligomycin in the presence of AX would be expected as mitochondrial membrane potential is higher in the presence of AX, while in the absence of AX, oligomycin is unable to increase membrane potential to the same level. Such an inhibition of respiration upon inactivation of complex V is referred to as "respiratory control ratio," an important measure of mitochondrial health when investigating isolated mitochondria [41], even though it should be pointed out that we used intact cells, where respiration during stimulation of complex V with ADP is not accessible, and the ratios are not comparable. Physiological effects of AX have been shown to include stimulation of β-oxidation for fatty acids [42,43]. This would be of considerable benefit in reducing obesity and metabolic syndrome in affluent societies. Much of the benefit of one of the most effective drugs for diabetes, metformin, has been attributed to activation of AMP-dependent kinase, which helps by reducing gluconeogenesis and driving oxidation of fat in muscle mitochondria [44]. The AX concentration upon which a significant benefit could be observed (200 nM, Fig. 1) is also well within the range that can be achieved with supplementation. A single oral dose of 10 mg AX resulted in a peak plasma concentration of ~130 nM, whereas a single dose of 100 mg AX resulted in a peak plasma concentration of ~470 nM, with half-lives in the order of days [25]. Similarly, daily consumption of 250 g of either wild or farmed salmon

(farmed salmon is fed synthetic AX to give it its natural coloring) lead to a plateau of ~50 nM AX in plasma after about 6 days [26].

Redox-sensitive GFP targeted to mitochondria could detect changes in the mitochondrial redox state even after short incubation with AX, where conventional methods failed. This indicates that roGFP is a powerful tool for measuring oxidative stress and redox balance at the organelle level. Targeting roGFP to mitochondria allowed us to detect changes in the mitochondrial redox state that were too small to affect the cytosol. Redox-sensitive GFP possibly interacts with a number of cellular enzymes and redox couples, but it is still unclear which determine the roGFP1 redox state to what extent. The reduction of roGFP1 is likely enzyme-dependent, as reductase and dehydrogenase inhibitors reduced or prevented reduction of the close cousin roGFP2 in the cytosol [20]. Conversely, oxidation of roGFP proceeded considerably faster when, compared to the isolated protein, it was expressed in cells, suggesting that the oxidation is also catalyzed by intracellular enzymes. In our hands, the response of roGFP1 to hydrogen peroxide was also significantly faster than previously reported [20]. RoGFP oxidation was observed immediately, and the maximum response in the cytosol was reached within 5 min (Fig. 6B).

The high sensitivity of roGFP to changes in organelle redox state suggests that it is a powerful tool to investigate the biochemistry of oxidative stress and redox balance at the organelle level. Accurate measurement of oxidative stress is an ongoing challenge, and despite the availability and ongoing development of a wide range of probes and methods, their correct use is often complicated (e.g., Ref. [45]) and/or cumbersome (e.g., Ref. [46]). The most widely employed method to "quantify" ROS, the conversion of dichlorodihydrofluorescein (H_2DCF) to DCF, requires a catalyst for H_2DCF to be oxidized by hydrogen peroxide and reacts indiscriminately with a variety of oxidizing factors, including light and itself [47,48].

RoGFP1 is a relatively new nondestructive and ratiometric sensor for cellular redox state [20,21] permitting a wide range of measurements previously impossible or extremely labor-intensive and therefore open to errors and artefacts. Experiments to establish the sensitivity of roGFP1 to various stressors and antioxidants are currently under way in our laboratory, but in our opinion, roGFP offers great promise for pin-point detection of oxidative stress. Targeting roGFP1 to subcellular structures allowed us to observe oxidative stress restricted to mitochondria without affecting the cytosol, demonstrating that changes in redox state and oxidative stress can be confined to cellular compartments. To understand cellular redox states, it might therefore be important to determine compartmental redox states independently. Furthermore, transgenic animals expressing roGFPs should be a valuable tool to test the efficacy of treatments aimed at reducing oxidative stress.

Acknowledgments

We express our deep gratitude to Prof. Jim Remington and his team for kindly providing the roGFP1 containing plasmids. Alexander Wolf was supported by a Postdoctoral Fellowship and grant from the Japan Society for the Promotion of Science.

Appendix A. Supplementary data

Supplementary data associated with this article can be found, in the online version, at doi:10.1016/j.jnutbio.2009.01.011.

References

[1] Lusis AJ. Atherosclerosis. Nature 2000;407:233–41.
[2] Schriner SE, Linford NJ, Martin GM, Treuting P, Ogburn CE, Emond M, et al. Extension of murine life span by overexpression of catalase targeted to mitochondria. Science 2005;308:1909–11.
[3] Serrano M, Blasco MA. Cancer and ageing: convergent and divergent mechanisms. Nat Rev Mol Cell Biol 2007;8:715–22.
[4] Houstis N, Rosen ED, Lander ES. Reactive oxygen species have a causal role in multiple forms of insulin resistance. Nature 2006;440:944–8.
[5] Brownlee M. Biochemistry and molecular cell biology of diabetic complications. Nature 2001;414:813–20.
[6] Beal MF. Bioenergetic approaches for neuroprotection in Parkinson's disease. Ann Neurol) 2003;53(Suppl 3):S39–47 [discussion S47-38].
[7] Dawson TM, Dawson VL. Molecular pathways of neurodegeneration in Parkinson's disease. Science 2003;302:819–22.
[8] Esposito E, Rotilio D, Di Matteo V, Di Giulio C, Cacchio M, Algeri S. A review of specific dietary antioxidants and the effects on biochemical mechanisms related to neurodegenerative processes. Neurobiol Aging 2002;23:719–35.
[9] Finkel T. Radical medicine: treating ageing to cure disease. Nat Rev Mol Cell Biol 2005;6:971–6.
[10] Kim MS, Park JY, Namkoong C, Jang PG, Ryu JW, Song HS, et al. Anti-obesity effects of alpha-lipoic acid mediated by suppression of hypothalamic AMP-activated protein kinase. Nat Med 2004;10:727–33.
[11] Klaus S, Pultz S, Thone-Reineke C, Wolfram S. Epigallocatechin gallate attenuates diet-induced obesity in mice by decreasing energy absorption and increasing fat oxidation. Int J Obes (Lond) 2005;29:615–23.
[12] Borra MT, Smith BC, Denu JM. Mechanism of human SIRT1 activation by resveratrol. J Biol Chem 2005;280:17187–95.
[13] Ridinger MH. Nutraceuticals: miracle or meme? Clin Pharmacol Ther 2007;82: 352–6.
[14] Kamel NS, Gammack J, Cepeda O, Flaherty JH. Antioxidants and hormones as antiaging therapies: high hopes, disappointing results. Cleve Clin J Med 2006;73:1049–56, 1058.
[15] Hansen JM, Go YM, Jones DP. Nuclear and mitochondrial compartmentation of oxidative stress and redox signaling. Annu Rev Pharmacol Toxicol 2006;46: 215–34.
[16] Thomson MJ, Puntmann V, Kaski JC. Atherosclerosis and oxidant stress: the end of the road for antioxidant vitamin treatment? Cardiovasc Drugs Ther 2007;21: 195–210.
[17] Vickers AJ. Which botanicals or other unconventional anticancer agents should we take to clinical trial? J Soc Integr Oncol 2007;5:125–9.
[18] Chinta SJ, Andersen JK. Reversible inhibition of mitochondrial complex I activity following chronic dopaminergic glutathione depletion in vitro: implications for Parkinson's disease. Free Radic Biol Med 2006;41:1442–8.
[19] Miyawaki A, Nagai T, Mizuno H. Engineering fluorescent proteins. Adv Biochem Eng Biotechnol 2005;95:1–15.
[20] Dooley CT, Dore TM, Hanson GT, Jackson WC, Remington SJ, Tsien RY. Imaging dynamic redox changes in mammalian cells with green fluorescent protein indicators. J Biol Chem 2004;279:22284–93.
[21] Hanson GT, Aggeler R, Oglesbee D, Cannon M, Capaldi RA, Tsien RY, et al. Investigating mitochondrial redox potential with redox-sensitive green fluorescent protein indicators. J Biol Chem 2004;279:13044–53.
[22] Hussein G, Sankawa U, Goto H, Matsumoto K, Watanabe H. Astaxanthin, a carotenoid with potential in human health and nutrition. J Nat Prod 2006;69:443–9.
[23] Higuera-Ciapara I, Felix-Valenzuela L, Goycoolea FM. Astaxanthin: a review of its chemistry and applications. Crit Rev Food Sci Nutr 2006;46:185–96.
[24] Gross GJ, Hazen SL, Lockwood SF. Seven day oral supplementation with Cardax (disodium disuccinate astaxanthin) provides significant cardioprotection and reduces oxidative stress in rats. Mol Cell Biochem 2006;283:23–30.
[25] Coral-Hinostroza GN, Ytrestoyl T, Ruyter B, Bjerkeng B. Plasma appearance of unesterified astaxanthin geometrical E/Z and optical R/S isomers in men given single doses of a mixture of optical 3 and 3'R/S isomers of astaxanthin fatty acyl diesters. Comp Biochem Physiol C Toxicol Pharmacol 2004;139:99–110.
[26] Rufer CE, Moeseneder J, Briviba K, Rechkemmer G, Bub A. Bioavailability of astaxanthin stereoisomers from wild (*Oncorhynchus* spp.) and aquacultured (*Salmo salar*) salmon in healthy men: a randomised, double-blind study. Br J Nutr 2007:1–7.
[27] Jha N, Jurma O, Lalli G, Liu Y, Pettus EH, Greenamyre JT, et al. Glutathione depletion in PC12 results in selective inhibition of mitochondrial complex I activity. Implications for Parkinson's disease. J Biol Chem 2000;275:26096–101.
[28] Ohsawa I, Ishikawa M, Takahashi K, Watanabe M, Nishimaki K, Yamagata K, et al. Hydrogen acts as a therapeutic antioxidant by selectively reducing cytotoxic oxygen radicals. Nat Med 2007;13:688–94.
[29] Reers M, Smith TW, Chen LB. J-aggregate formation of a carbocyanine as a quantitative fluorescent indicator of membrane potential. Biochemistry 1991;30: 4480–6.
[30] Schwarzer C, Illek B, Suh JH, Remington SJ, Fischer H, Machen TE. Organelle redox of CF and CFTR-corrected airway epithelia. Free Radic Biol Med 2007;43: 300–16.
[31] Meyer AJ, Brach T, Marty L, Kreye S, Rouhier N, Jacquot JP, et al. Redox-sensitive GFP in *Arabidopsis thaliana* is a quantitative biosensor for the redox potential of the cellular glutathione redox buffer. Plant J 2007;52:973–86.
[32] Choksi KB, Nuss JE, Boylston WH, Rabek JP, Papaconstantinou J. Age-related increases in oxidatively damaged proteins of mouse kidney mitochondrial electron transport chain complexes. Free Radic Biol Med 2007;43:1423–38.
[33] Manabe E, Handa O, Naito Y, Mizushima K, Akagiri S, Adachi S, et al. Astaxanthin protects mesangial cells from hyperglycemia-induced oxidative signaling. J Cell Biochem 2007.
[34] Jyonouchi H, Sun S, Iijima K, Gross MD. Antitumor activity of astaxanthin and its mode of action. Nutr Cancer 2000;36:59–65.

[35] Hayashi J, Ohta S, Kikuchi A, Takemitsu M, Goto Y, Nonaka I. Introduction of disease-related mitochondrial DNA deletions into HeLa cells lacking mitochondrial DNA results in mitochondrial dysfunction. Proc Natl Acad Sci U S A 1991;88:10614–8.
[36] Lyamzaev KG, Izyumov DS, Avetisyan AV, Yang F, Pletjushkina OY, Chernyak BV. Inhibition of mitochondrial bioenergetics: the effects on structure of mitochondria in the cell and on apoptosis. Acta Biochim Pol 2004;51:553–62.
[37] Han YH, Kim SH, Kim SZ, Park WH. Antimycin A as a mitochondria damage agent induces an S phase arrest of the cell cycle in HeLa cells. Life Sci 2008;83:346–55.
[38] Yamamoto N, Sawada H, Izumi Y, Kume T, Katsuki H, Shimohama S, et al. Proteasome inhibition induces glutathione synthesis and protects cells from oxidative stress: relevance to Parkinson disease. J Biol Chem 2007;282:4364–72.
[39] Schwerzmann K, Cruz-Orive LM, Eggman R, Sanger A, Weibel ER. Molecular architecture of the inner membrane of mitochondria from rat liver: a combined biochemical and stereological study. J Cell Biol 1986;102:97–103.
[40] Foss BJ, Sliwka HR, Partali V, Cardounel AJ, Zweier JL, Lockwood SF. Direct superoxide anion scavenging by a highly water-dispersible carotenoid phospholipid evaluated by electron paramagnetic resonance (EPR) spectroscopy. Bioorg Med Chem Lett 2004;14:2807–12.
[41] Ainscow EK, Brand MD. Internal regulation of ATP turnover, glycolysis and oxidative phosphorylation in rat hepatocytes. Eur J Biochem 1999;266:737–49.
[42] Aoi W, Naito Y, Takanami Y, Ishii T, Kawai Y, Akagiri S, et al. Astaxanthin improves muscle lipid metabolism in exercise via inhibitory effect of oxidative CPT I modification. Biochem Biophys Res Commun 2008;366:892–7.
[43] Ikeuchi M, Koyama T, Takahashi J, Yazawa K. Effects of astaxanthin in obese mice fed a high-fat diet. Biosci Biotechnol Biochem 2007;71:893–9.
[44] Zhou G, Myers R, Li Y, Chen Y, Shen X, Fenyk-Melody J, et al. Role of AMP-activated protein kinase in mechanism of metformin action. J Clin Invest 2001;108:1167–74.
[45] Johnson-Cadwell LI, Jekabsons MB, Wang A, Polster BM, Nicholls DG. 'Mild Uncoupling' does not decrease mitochondrial superoxide levels in cultured cerebellar granule neurons but decreases spare respiratory capacity and increases toxicity to glutamate and oxidative stress. J Neurochem 2007;101:1619–31.
[46] Arneson KO, Roberts Jr LJ. Measurement of products of docosahexaenoic acid peroxidation, neuroprostanes, and neurofurans. Methods Enzymol 2007;433:127–43.
[47] Wrona M, Wardman P. Properties of the radical intermediate obtained on oxidation of 2′,7′-dichlorodihydrofluorescein, a probe for oxidative stress. Free Radic Biol Med 2006;41:657–67.
[48] Wrona M, Patel KB, Wardman P. The roles of thiol-derived radicals in the use of 2′,7′-dichlorodihydrofluorescein as a probe for oxidative stress. Free Radic Biol Med 2008;44:56–62.